

Electronic structure determination and dynamical properties of iron (II)guanosine5' monophosphate complex via mossbauer and magnetic susceptibility measurements

J. R. Alabart, V. Moreno, A. Labarta, J. Tejada, and E. Molins

Citation: *The Journal of Chemical Physics* **92**, 6131 (1990); doi: 10.1063/1.458336

View online: <http://dx.doi.org/10.1063/1.458336>

View Table of Contents: <http://scitation.aip.org/content/aip/journal/jcp/92/10?ver=pdfcov>

Published by the [AIP Publishing](#)

Articles you may be interested in

[The radiationinduced oxidation and reduction of guanine: Electron spin resonance–electron nuclear double resonance studies of irradiated guanosine cyclic monophosphate](#)

J. Chem. Phys. **90**, 1448 (1989); 10.1063/1.456086

[Electronic structure determination of iron\(II\) phthalocyanine via magnetic susceptibility and Mössbauer measurements](#)

J. Chem. Phys. **80**, 444 (1984); 10.1063/1.446469

[Properties of binary tin chalcogenides determined by Mossbauer spectroscopy](#)

J. Chem. Phys. **61**, 5017 (1974); 10.1063/1.1681841

[Magnetic Properties of Hydrogen Fluoride. II. Susceptibility](#)

J. Chem. Phys. **36**, 2786 (1962); 10.1063/1.1732367

[A Determination of the Magnetic Susceptibilities of Certain Inorganic Complex Compounds](#)

J. Chem. Phys. **6**, 462 (1938); 10.1063/1.1750292



Electronic structure determination and dynamical properties of iron (II)-guanosine-5'-monophosphate complex via mossbauer and magnetic susceptibility measurements

J. R. Alabart and V. Moreno

Departamento de Química, Universidad de Barcelona, Imperial Tàrraco 1, Tarragona 43005, Spain

A. Labarta^{a)} and J. Tejada

Departamento de Física Fundamental, Universidad de Barcelona, Diagonal 645, Barcelona 08028, Spain

E. Molins

Institut de Ciència de Materials, Martí i Franquès s/n, Barcelona 08028, Spain

(Received 12 December 1989; accepted 8 February 1990)

The electronic structure of the ferrous ion in the Fe(II)-5'-GMP complex has been determined by means of least-squares fittings of the temperature dependence of both the quadrupole splitting and the magnetic susceptibility experimental data, using a crystal-field approximation. The resulting low lying energy levels in order of increasing energy were 5B_2 , 1A_1 , 5E , and 3E , but after applying the rhombic perturbation, the rhombic-split 5E term became the ground state due to a quite large rhombic distortion $D = -2236 \text{ cm}^{-1}$. The set of crystal-field parameters obtained from the fit has been correlated with the molecular structure of the Fe(II)-5'-GMP derivative. The great value of the e_2 parameter is indicative of a strong N_7 -Fe interaction while the values of the e_3 parameter and the rhombic distortion are in agreement with a large distortion in the octahedron plane. Finally, the Debye temperature of the solid has been derived from the thermal variation of the Lamb-Mössbauer factor and has been used to calculate the second-order Doppler shift of the ferrous cation which, together with the assumption of a linear temperature dependence for the intrinsic isomer shift, reproduces the isomer shift experimental data.

I. INTRODUCTION

In the last three decades, the interaction of metal ions with nucleic acid constituents has been actively investigated in view of the importance of metal ions in the biochemistry of nucleic acids.¹ Thus, it was early discovered that iron was a component of tobacco mosaic virus DNA and that it was strongly bonded to complexing sites in the nucleic acid.² Further, Fe(II) ions act as cofactors in the degradation of DNA by bleomycin, a glycopeptide antibiotic used for the treatment of selected human neoplastic diseases which is commonly used with *cis*-[Pt(NH₃)₂Cl₂], another effective antitumor drug that produces its effects via interaction with the nucleic acids of tumor cells.³ On the other hand, heavy metal ions acting as environmental pollutants can cause pernicious effects. Finally, another interesting point is the use of a diversity of metal ions and metal compounds as probes of the function of nucleic acids and aids in the separation, purification, and structural investigations of these biomolecules.⁴

Many complexes of metal ions with nucleic acid constituents have been studied by x-ray diffraction,⁵ but in spite of this rapid growth in x-ray structural information about the binding of metal ions to nucleic acids components, there are numerous cases where structural conclusions must be based on less direct methods, usually because suitable crys-

tals cannot be obtained. A notable example of this is provided by the iron derivatives of nucleotides. The only two x-ray structures of iron (II)-nucleotide systems reported so far are those of Goodgame *et al.*, corresponding to the complexes [Fe(5'-IMP)(H₂O)₅]·2H₂O⁶ and [Fe(5'-GMP)(H₂O)₅]·3H₂O⁷. In these compounds, the iron ion is octahedrally coordinated to five water molecules and to the N₇ position on the purine moiety (see Fig. 1). In the case of the 5'-IMP derivative, the ⁵⁷Fe Mössbauer measurements have been correlated with the molecular structure⁸ and the electronic structure for the iron cations has been determined from the temperature dependence of the quadrupole Mössbauer splitting.⁹

As part of our systematic study of the Fe(II) derivatives of the major purine and pyrimidine nucleotides, in this paper we discuss magnetic susceptibility and Mössbauer measurements on the Fe(II)-5'-GMP system which have been simultaneously used to determine the crystal field parameters and the electronic structure for the Fe(II) ions, using the ligand field approximation introduced by Eicher and Trautwein.¹⁰

As has been pointed out by Huynh *et al.*,¹¹ Mössbauer temperature-dependent quadrupole splitting data alone are insufficient to uniquely determine the ordering and splitting of the low-lying levels of Fe(II). In this way, we have used both the temperature dependence of the Mössbauer quadrupole splitting and the magnetic susceptibility measurements to determine the electronic structure of the Fe(II) ion. A set of crystal field parameters were found to simulate correctly

^{a)} Author to whom all correspondence should be addressed.

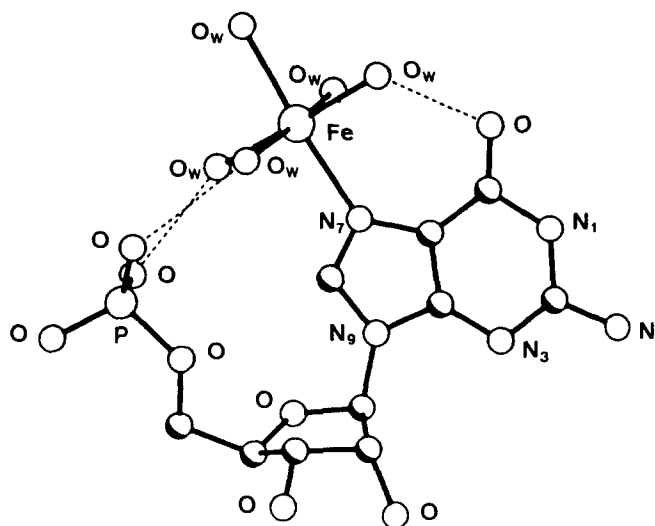


FIG. 1. Molecular structure of $[\text{Fe}(5'\text{-GMP})(\text{H}_2\text{O})_5] \cdot 3\text{H}_2\text{O}$ (Ref. 7). Broken lines indicate intramolecular hydrogen bonds.

the temperature dependence of both the quadrupole splitting and the magnetic susceptibility data. This set of crystal-field parameters obtained from the fitting procedure have been correlated with the known molecular structure of the $\text{Fe}(\text{II})$ -5'-GMP complex, and along with those determined for the analogous $\text{Fe}(\text{II})$ -5'-IMP derivative, they will serve to establish comparisons with those of other $\text{Fe}(\text{II})$ -ribonucleotide complexes whose x-ray structure is not known yet. The resulting electronic structure, after applying the rhombic perturbation, has low-lying 5E , 5B_2 , and 1A_1 levels with a quite large rhombic distortion ($\sim 2200 \text{ cm}^{-1}$). This electronic structure is the same one found in some important biological molecules such as deoxygenated sperm whale myoglobin and deoxygenated human hemoglobin.^{11,12}

It has been this similarity in the electronic structures which has prompted us to start a study about the dynamical properties of the $\text{Fe}(\text{II})$ -5'-GMP molecule. From the temperature dependence of the Lamb-Mössbauer factor, we have determined the Debye temperature of the solid ($\theta_D = 185 \text{ K}$) and this has been employed to calculate the second-order Doppler shift of the $\text{Fe}(\text{II})$ ions which along with a linear temperature dependence for the intrinsic isomer shift leads to a good fitting of the experimental data.

II. EXPERIMENTAL PROCEDURE

A. Synthesis

The preparation of the $\text{Fe}(\text{II})$ -5'-GMP derivative was carried out under an atmosphere of argon and the water used was deoxygenated by passing argon through the liquid for at least 2 h. A solution of $\text{Na}_25\text{-GMP}$ (disodium salt of guanosine-5'-monophosphate) in water was added to one with the stoichiometric amount of $\text{FeSO}_4 \cdot 7\text{H}_2\text{O}$ [iron (II) sulphate heptahydrate]. An immediate, flocculent white precipitate was obtained. This precipitate was filtered off under argon,

washed with deoxygenated water, and dried under P_2O_5 in a drybox. Once obtained in dry state, the product seems to be reasonably stable to air oxidation. Analytical results were consistent with the formulation $\text{Fe}(5'\text{-GMP}) \cdot 7\text{H}_2\text{O}$; calc. (%) C, 22.10; H, 4.79; N, 12.89; Fe, 10.28. Found (%) C, 22.17; H, 4.85; N, 12.82; Fe, 10.00.

B. Experimental techniques

The analyses of carbon, hydrogen, and nitrogen were carried out on a Carlo Erba model 1106 microanalyzer and on a Perkin-Elmer 240.B. The iron content was determined by atomic absorption spectroscopy in an Instrumentation Laboratory Inc. model IL551 spectrometer. The working conditions were $\lambda = 248.3 \text{ nm}$ and slit = 0.3 nm with an acetylene-air oxidant flame.

The Fourier transform-infrared (FT-IR) spectra of the $\text{Fe}(\text{II})$ -5'-GMP complex and the $\text{Na}_25\text{-GMP}$ salt were recorded on KBr pellets in a Nicolet model 5ZDX spectrometer in the $4000\text{--}400 \text{ cm}^{-1}$ range with a spectral resolution of 2 cm^{-1} .

${}^{57}\text{Fe}$ Mössbauer spectra were carried out using a constant-acceleration spectrometer in the 71–300 K temperature range. The low-temperature results were obtained with a liquid nitrogen cryostat. The spectrometer was equipped with a source of 10 mCi of ${}^{57}\text{Co}$ in a rhodium matrix which was maintained at room temperature and was calibrated with metallic iron.

Magnetic susceptibility was measured with a Faraday balance in the 14–300 K temperature range at a magnetic field of $\sim 2500 \text{ G}$. Cooling was achieved using a commercial closed-cycle helium-gas heat pump and a gold-chromel thermocouple served to measure the sample temperature with an accuracy $\sim 0.1 \text{ K}$. The balance was calibrated by using $\text{CoHg}(\text{NCS})_4$. The sensitivity of the system is between $10^{-5}\text{--}10^{-6} \text{ emu}$ depending on the field strength.

III. RESULTS

A. FT-IR

In the spectral region of $4000\text{--}2700 \text{ cm}^{-1}$, due to the presence of the strong intramolecular hydrogen bonding of the free 5'-GMP ligand and its metal derivatives,¹³ it is difficult to draw any conclusions on the nature of the metal-ligand interaction.

The bands and their possible assignments in the $1800\text{--}400 \text{ cm}^{-1}$ range are given in Table I. The tentative assignments are based on those made by Tajmir-Riahi and Theophanides for a series of other N_7 -guanine-bonded metal complexes.¹³ The free 5'-GMP shows a broad and strong absorption band at 1694.3 cm^{-1} attributable to the stretching vibration of $\text{C}_6=\text{O}$ which does not show any considerable displacement. This is mainly due to the participation of the O_6 atom of 5'-GMP in hydrogen bonding with one of the coordinated water molecules in the complex. The bending (scissoring) motion NH_2 of the free ligand at 1663.0 cm^{-1} gains intensity and splits into two components at 1647.2 and 1638.5 cm^{-1} . This shift to lower frequencies would be due to a weakening of the $\text{O} \cdots \text{H}-\text{N}-\text{H} \cdots \text{O}$ hydrogen bonding to the phosphate group in the structure of the $\text{Fe}(\text{II})$ -5'-

TABLE I. FT-IR bands (cm^{-1}) and possible assignments for $\text{Na}_2 5'\text{-GMP}$ salt and $[\text{Fe}(5'\text{-GMP})(\text{H}_2\text{O})_5] \cdot 2\text{H}_2\text{O}$ complex in the $1700\text{--}800\text{ cm}^{-1}$ range.

$\text{Na}_2 5'\text{-GMP}$	$[\text{Fe}(5'\text{-GMP})(\text{H}_2\text{O})_5] \cdot 2\text{H}_2\text{O}$	Possible assignments ^a
1694.3 br,vs ^b	1693.3 s	$\nu\text{C}_6 = \text{O} > \nu\text{C}_6 = \text{C}_5$
1663.0 sh,s	1647.2 sh,s	$\delta\text{NH}_2 > \nu\text{C}_2\text{--N}_2$
	1638.5 s	
1603.0 s	1610.2 sh,s	$\nu\text{C}_4\text{--N}_3 > \nu\text{C}_4\text{--C}_5 > \nu\text{C}_5\text{--N}_7$
1589.2 sh,s	1578.6 sh,m	$\nu\text{C}_5\text{--C}_4 > \delta\text{N}_1\text{--H} > \nu\text{C}_6\text{--N}_1$
1535.7 s	1535.1 w	$\nu\text{C}_4\text{--N}_9 > \nu\text{C}_6 = \text{O} > \nu\text{C}_2\text{--N}_1$
1483.0 s	1483.7 w	$\delta\text{C}_8\text{--H} > \nu\text{C}_8\text{--N}_7$
	1463.7 sh,vw	
1412.5 m	1414.4 w	$\delta\text{CH} + \delta\text{CH}_2$
1360.8 s	1358.0 w	$\nu(\text{pyrimidine ring})$
1330.8 sh,m	1318.7 sh,vw	$\nu\text{C}_8\text{--N}_9 > \nu\text{C}_8\text{--N}_7 > \delta\text{N}_1\text{--H} > \nu\text{C}_2\text{--N}_2$
1254.2 sh,m	1261.0 w	$\nu\text{C}_6\text{--N}_1 > \nu\text{C}_5\text{--N}_7$
1236.0 m	1235.8 w	
1209.5 sh,w	Masked by phosphate bands	$\delta\text{C}_8\text{--H} > \nu\text{C}_8\text{--N}_7$
1180.5 s	Masked by phosphate bands	$\nu\text{C}_8\text{--N}_7 > \nu\text{N}_9\text{--sugar} > \nu\text{C}_4\text{--N}_3$
1119.8 sh,vs	1107.2 vs	$\nu\text{C--O}$ of the sugar ring
1078.3 br,vs	1083.8 vs	νPO_3^{2-} degenerate
975.9 vs	992.4 s	νPO_3^{2-} symmetric
805.1 m	800.8 w	$\nu\text{P--O}$

^a Tentative assignments based on Ref. 13.^b s = strong, vs = very strong, m = medium, w = weak, vw = very weak, sh = shoulder, br = broad.

GMP complex. The band at 1603.0 cm^{-1} corresponding to skeletal vibrations shifts to 1610.2 cm^{-1} . This shift is due to the inductive effect of the $\text{Fe}(\text{II})$ ion bound to N_7 since it causes less electron delocalization and finally less contribution to the skeletal vibrations of the ring system.

One of the most common changes observed in the vibrational spectra of N_7 -bonded metal complexes of the $5'\text{-GMP}$ nucleotide¹³ is related with the modification of the band at 1483.0 cm^{-1} which involves primarily the five membered ring $\text{C}_8\text{--H}$ bending and the $\text{N}_7\text{--C}_8$ stretching frequencies. This band splits into two absorption bands at 1483.7 and 1463.7 (sh) cm^{-1} . Nonetheless, the two absorption bands with medium intensities at 1330.8 and 1254.2 cm^{-1} in the spectrum of $5'\text{-GMP}$ mainly assigned to $\text{N}_7\text{--C}_8$, $\text{C}_8\text{--N}_9$, and $\text{N}_7\text{--C}_5$ stretching frequencies do not appear as a doublet.¹³ The related band at 1209.5 cm^{-1} has been masked by the broad absorption bands corresponding to the phosphate moiety.

Finally, the lack of splitting and major shifting of the phosphate-moiety bands at 1078.3 , 975.9 , and 805.1 cm^{-1} is indicative of the indirect $\text{Fe}(\text{II})$ -phosphate interaction through hydrogen-bonded water molecules.

B. Mössbauer spectroscopy

The Mössbauer spectra of the $[\text{Fe}(5'\text{-GMP})(\text{H}_2\text{O})_5] \cdot 2\text{H}_2\text{O}$ complex in the studied temperature range are well described by the superposition of two quadrupolar splittings, corresponding to $\text{Fe}(\text{II})$ and $\text{Fe}(\text{III})$ oxidation states. The spectrum recorded at room temperature, which is representative of the obtained spectra, is shown in Fig. 2. The iron(III) oxidation state is due to partial oxidation of the compound during the synthetic process, as has

been noted previously. In any case, as can be seen in Fig. 2, the relative amount of $\text{Fe}(\text{III})$ with respect to the total amount is less than 10%. The Mössbauer parameters listed in Table II are determined fitting the spectra by a least-squares method assuming that the two Lorentzian lines of the quadrupole doublets have the same intensity and width. Only the parameters relative to the $\text{Fe}(\text{II})$ ion are presented since the quadrupole doublet corresponding to $\text{Fe}(\text{III})$ will be considered as an impurity.

The isomer shift values for the $\text{Fe}(\text{II})$ - $5'\text{-GMP}$ derivative are quite similar to those previously reported for the analogous $\text{Fe}(\text{II})$ - $5'\text{-IMP}$ complex⁸ and along with the qua-

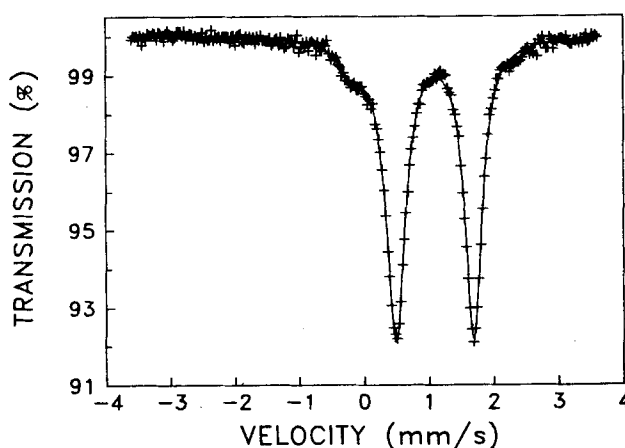
FIG. 2. Mössbauer absorption spectrum of $[\text{Fe}(5'\text{-GMP})(\text{H}_2\text{O})_5] \cdot 2\text{H}_2\text{O}$ at room temperature.

TABLE II. ^{57}Fe Mössbauer parameters for $[\text{Fe}(\text{5'-GMP})(\text{H}_2\text{O})_5] \cdot 2\text{H}_2\text{O}$.

$T(\text{K})$	$\delta^a (\text{mm s}^{-1})$	$\Delta E_Q (\text{mm s}^{-1})$	$\Gamma^b (\text{mm s}^{-1})$	$-\ln(\Gamma \cdot I)$
71.6	1.37 ± 0.02	1.93 ± 0.03	0.21 ± 0.01	3.49 ± 0.08
85.0	1.36 ± 0.02	1.90 ± 0.03	0.20 ± 0.01	3.52 ± 0.11
110.2	1.35 ± 0.02	1.81 ± 0.03	0.18 ± 0.01	3.63 ± 0.07
150.0	1.33 ± 0.02	1.68 ± 0.03	0.19 ± 0.01	3.75 ± 0.10
180.0	1.31 ± 0.02	1.57 ± 0.03	0.16 ± 0.01	3.92 ± 0.08
210.2	1.30 ± 0.02	1.49 ± 0.03	0.18 ± 0.01	4.03 ± 0.11
240.1	1.28 ± 0.02	1.40 ± 0.03	0.16 ± 0.01	4.16 ± 0.12
300.0	1.24 ± 0.02	1.27 ± 0.04	0.17 ± 0.01	4.37 ± 0.13

^a Relative to metallic iron.^b Linewidth at half height.

drupole splitting values, they are consistent with Fe(II) high spin electronic configuration. All the Mössbauer parameters are temperature dependent, especially and most significantly the quadrupolar splitting.

C. Magnetic susceptibility

In order to get only the Fe(II) ion contribution to the total magnetic susceptibility of the sample, we have subtracted the susceptibility corresponding to the Fe(III) fraction, which have been estimated by Mössbauer spectroscopy ($9.7 \pm 0.5\%$), assuming that Fe(III) is in a high-spin 6S_1 configuration. The diamagnetic correction has been calculated by means of the Pascal's constants¹⁴ and it has been estimated to be $238.7 \times 10^{-6} \text{ cm}^3 \text{ mol}^{-1}$. The corrected reciprocal molar magnetic susceptibility follows the Curie-Weiss law, as can be seen in Fig. 3, with a Curie constant $C = 3.09 \pm 0.02 \text{ cm}^3 \text{ K mol}^{-1}$ which corresponds to a paramagnetic moment of $\mu = 4.97 \pm 0.03 \mu_B$, and a Curie temperature of $\theta = 3.5 \pm 0.5 \text{ K}$. The general behavior of the reciprocal susceptibility and in particular the Curie tempera-

ture are indicative that nonmagnetic interactions are present among the Fe(II) cations such as should be expected from the molecular structure.⁷ The paramagnetic moment is consistent with a high-spin electronic state of the Fe(II) ions and it is very close to the spin-only value ($\mu = 4.90 \mu_B$), indicating a small orbital contribution. On the other hand, this value is much smaller than those reported in the literature for other octahedral Fe(II) compounds¹⁵ and this may be attributed to a greater local distortion around the Fe(II) ions.

IV. ELECTRONIC ENERGY LEVELS OF FERROUS IONS IN THE Fe(II)-5'-GMP COMPLEX

With the aim of obtaining more information about the interaction between the Fe(II) ion and the 5'-GMP ribonucleotide, the electronic structure of the Fe(II) ions have been calculated in the scope of a single-point crystal-field model. In this model, the low-lying energy levels of the Fe(II) ion result from the diagonalization of the Hamiltonian

$$H^0 = H_{ee} + H_{cf} \quad (1)$$

in the basis of the $3d^6$ configuration, where H_{ee} is the Coulomb Hamiltonian and H_{cf} accounts for the crystal-field potential, which assuming a C_{2v} symmetry for the Fe(II) position in the Fe(II)-5'-GMP complex, can be expanded in terms of the V_{lm} operators¹⁰

$$H_{cf} = (2/7)^{1/2} (\epsilon_3 - \epsilon_2 - \epsilon_1) V_{20} + [(70)^{1/2}/70] \times (\epsilon_3 + 6\epsilon_2 + 8\epsilon_1) V_{40} + (\epsilon_3/2) (V_{44} + V_{4-4}) + (7/3)^{1/2} D (V_{22} + V_{2-2}), \quad (2)$$

where the crystal-field parameters ϵ_i ($i = 1, 2, 3$) and D are the electronic splittings of the 3D energy levels (see Fig. 4).^{10,16} For realistic values of the crystal-field parameters, the wave functions having the lowest energy^{10,11,16} are 3E_g , $^3A_{2g}$, $^5A_{1g}$, 5E_g , $^3B_{2g}$, $^5B_{2g}$, and $^1A_{1g}$. In this subset of eigenstates, the total Hamiltonian H ,

$$H = H^0 + H_{SO} + H_m, \quad (3)$$

is re-diagonalized, where H_{SO} represents the spin-orbit coupling and H_m stands for the interaction with an external magnetic field in the case of magnetic measurements.

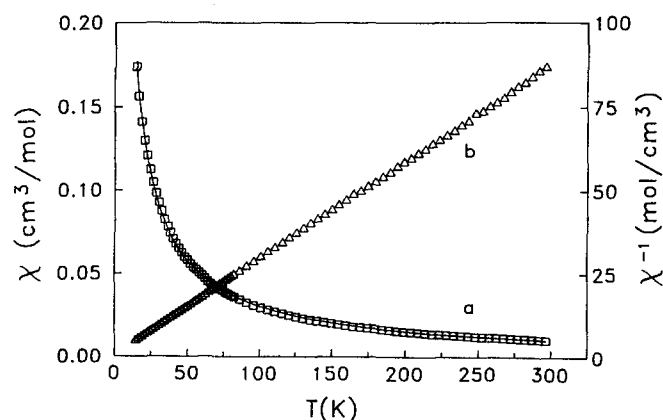
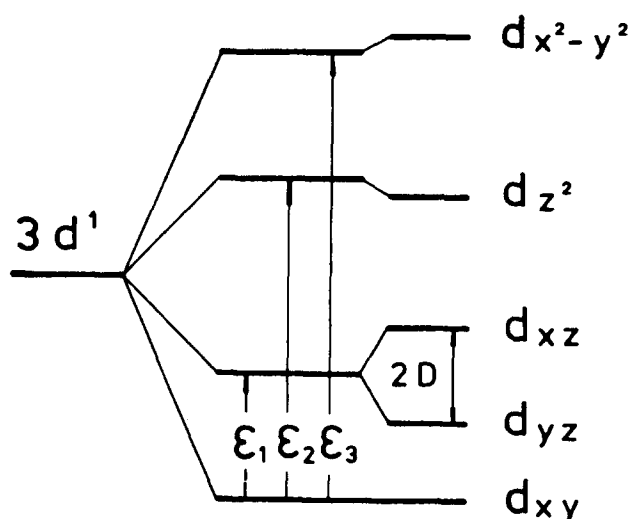


FIG. 3. Temperature dependence of the corrected magnetic susceptibility of Fe(II) ion in the $[\text{Fe}(\text{5'-GMP})(\text{H}_2\text{O})_5] \cdot 2\text{H}_2\text{O}$ complex (curve a). The solid line gives the best theoretical fit to the experimental data and it is obtained by the least-squares fit described in the text. Curve b is the reciprocal corrected magnetic susceptibility which follows the Curie-Weiss law with a Curie constant $C = 3.09 \pm 0.02 \text{ cm}^3 \text{ K mol}^{-1}$ and a Curie temperature of $\theta = 3.5 \pm 0.5 \text{ K}$.

FIG. 4. Splitting of the 3D levels in a C_{2v} symmetry environment.

A. Magnetic susceptibility

The average magnetization \mathbf{M} at a temperature T can be calculated by using the following equations:

$$m_i = -\partial E_i / \partial |\mathbf{B}|, \quad (4)$$

$$\langle \mathbf{M} \rangle_T = \sum_i m_i e^{-E_i/k_B T} / \sum_i e^{-E_i/k_B T}, \quad (5)$$

where \mathbf{B} is the external magnetic field and E_i and m_i are the i th eigenvalue and dipolar magnetic moment, respectively. The molar susceptibility can be expressed as

$$\chi_M = \frac{N_A \langle \mathbf{M} \rangle_T}{|\mathbf{B}|}, \quad (6)$$

where N_A is Avogadro's number.

B. Quadrupole interaction

The hyperfine interaction of a quadrupole nuclear moment Q with an electric field gradient (EFG) can be described by the following Hamiltonian¹⁷:

$$H_Q = \frac{e^2 Q}{4I(2I-1)} [q_{zz}(3I_z^2 - I^2) + \frac{1}{2}(q_{xx} - q_{yy})(I_+^2 + I_-^2)], \quad (7)$$

where I is the nuclear spin and q_{ii} are the principal axis components of the EFG tensor.

In the case of the nuclear levels of the ^{57}Fe between which takes place the Mössbauer transition, the eigenvalues of H_Q are given to first order by

$$E_Q(T) = \pm \frac{1}{4} e^2 Q q_{zz} (1 + \frac{1}{3} \eta_z^2)^{1/2}, \quad (8)$$

where $\eta_z = (q_{yy} - q_{xx})/q_{zz}$ is the asymmetry parameter. The EFG terms q_{ii} which are given by

$$q_{ii} = (1 - \gamma_\infty) q_{ii}^{\text{latt}} + (1 - R) \langle q_{ii}^{\text{ion}} \rangle_T \quad (9)$$

have two contributions: lattice (q_{ii}^{latt}) and valence electronic (q_{ii}^{ion}) contributions. In Eq. (8), R and γ_∞ parameters are the Sternheimer shielding and antishielding factors, which represent the electron polarization induced in the core and valence electron shells.¹⁸

The lattice contribution (q_{ii}^{latt}) does not depend on temperature and can be expressed in terms of the one-electron splitting of the 3D energy levels ϵ_i (Fig. 4)¹²

$$q_{zz}^{\text{latt}} = \frac{2(\epsilon_3 - \epsilon_2 - \epsilon_1)}{\langle r^2 \rangle}, \quad (10)$$

$$q_{yy}^{\text{latt}} - q_{xx}^{\text{latt}} = 0. \quad (11)$$

The valence electron contribution to the EFG tensor can be written as¹⁰

$$\langle q_{ii}^{\text{ion}} \rangle = \frac{\sum_v \langle v | q_{ii} | v \rangle e^{-E_v/k_B T}}{\sum_v e^{-E_v/k_B T}}, \quad (12)$$

where $|v\rangle$ are the eigenvectors of the total valence electron Hamiltonian ($H^0 + H_{\text{SO}}$).

C. Fitting procedure and discussion

The corrected molar susceptibility $\chi_M(T)$ and the quadrupolar splitting $\Delta E_Q(T)$ experimental data have been fitted by a least-squares method to the functions given by Eqs. (6) and (8). The adjustable parameters used in this procedure are the ϵ_i ($i = 1, 2, 3$) and D crystal-field parameters, the covalency factor α^2 , and the q_{zz}^{latt} value.

The crystal-field parameters ϵ_i ($i = 1, 2, 3$) and D determine fully the symmetry and intensity of the H_{cf} Hamiltonian (see Fig. 4).^{10,16} The covalency parameter α^2 takes into account the covalency degree of the iron (II) ions in the complex and it quantifies the reduction of the free ion spin-orbit coupling constant λ_0 ($\lambda = \alpha^2 \lambda_0$). Finally, the q_{zz}^{latt} parameter is the lattice contribution to the zz component of the EFG tensor.

The magnetic moment of 4.97 BM is typical of high spin ($S = 2$) ferrous compounds and it is slightly greater than the spin-only value of 4.90 BM. Hence, the symmetry of the crystal field must be low since the orbital angular moment is practically quenched and the ground state must, therefore, be either 5B_2 or 5E . Nonetheless, a well-isolated 5B_2 or 5E ground state would give a value of ΔE_Q of approximately 4.5 mm s^{-1} , which is much greater than the obtained experimental values, however, considering that the 5E state produces EFG components opposite to those produced by the 5B_2 level, any mixture of 5E with 5B_2 states will reduce the quadrupole splitting. Taking into account these considerations, we first selected sets of ϵ_i and D values such that they were in accordance with the reasons exposed above. In this way, an energy level configuration was found to give a good agreement for both magnetic susceptibility and quadrupole splitting experimental data. The results of the fitting procedure are summarized in Table III and the theoretical quadrupole splittings and magnetic susceptibilities are compared with the experimental data in Figs. 5 and 3, respectively. The resulting energy diagram of the low-lying electronic states of ferrous ion is shown in Fig. 6.

The values obtained for the crystal-field parameters ϵ_i

TABLE III. Least-squares parameters from the simultaneous fit of magnetic susceptibility and Mössbauer experimental data (left column) and obtained values of the energy of low-lying multielectron terms corresponding to the d^6 configuration after applying the rhombic perturbation (right column).

$\epsilon_1(\text{cm}^{-1}) = 2139 \pm 50$	$^5A_g(\text{cm}^{-1}) = 0^a$
$\epsilon_2(\text{cm}^{-1}) = 11\,377 \pm 50$	$^5B_2(\text{cm}^{-1}) = 98 \pm 10$
$\epsilon_3(\text{cm}^{-1}) = 17\,747 \pm 30$	$^1A_1(\text{cm}^{-1}) = 297 \pm 35$
$D(\text{cm}^{-1}) = -2236 \pm 100$	$^3E_g(\text{cm}^{-1}) = 833 \pm 35$
$\alpha^2 = 0.88$	$^3E_g(\text{cm}^{-1}) = 2830 \pm 100$
$\lambda(\text{cm}^{-1}) = 80$	$^5E_g(\text{cm}^{-1}) = 4571 \pm 100$
$\gamma_\infty = 1.8 \times 10^{-5b}$	

^a Arbitrarily fixed; a and b subscripts refer to levels resulting from the rhombic splitting.

^b Coefficient of the lattice contribution.

and D can be correlated with the molecular structure of the Fe(II)-5'-GMP complex.⁷ The energy ϵ_2 of the d_z^2 orbital depends very sensitively on the binding strength of the N₇ nitrogen of the purine moiety. Thus, a stronger Fe(II)-N₇ bond in the Fe(II)-5'-GMP complex than in the two iron binding sites of the analogous Fe(II)-5'-IMP derivative leads to a greater value of ϵ_2 (see Table IV). The corresponding energy gap ϵ_3 is a measure of the bond strength between the Fe(II) cation and the four water molecules in the plane of the octahedron. The value of ϵ_3 for the Fe(II)-5'-GMP complex is closer to those found in such systems as deoxygenated human hemoglobin and sperm whale myoglobin than those of the Fe(II)-5'-IMP derivative. Therefore, it seems that the ferrous ions in the Fe(II)-5'-GMP complex are in a lower planar disposition than in the related Fe(II)-5'-IMP one, and this fact is also reflected in a greater rhombic distortion, which can be attributed to the shorter Fe-N₇ bond in the Fe(II)-5'-GMP derivative.

The final electronic structure of the ferrous ions in the Fe(II)-5'-GMP system is very similar to those found in bio-

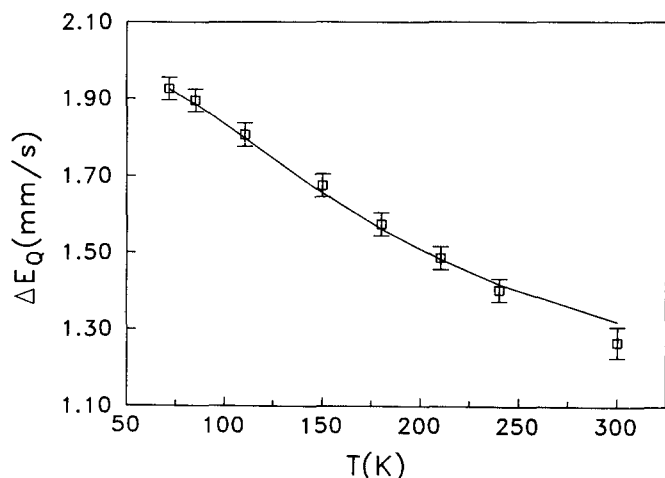


FIG. 5. Temperature dependence of the quadrupole splitting of Fe(II) ion in the $[\text{Fe}(5'\text{-GMP})(\text{H}_2\text{O})_5] \cdot 2\text{H}_2\text{O}$ complex. The solid line represents the best fit to the experimental data of $\Delta E_Q(T)$ and it is obtained by the least-squares fit described in the text.

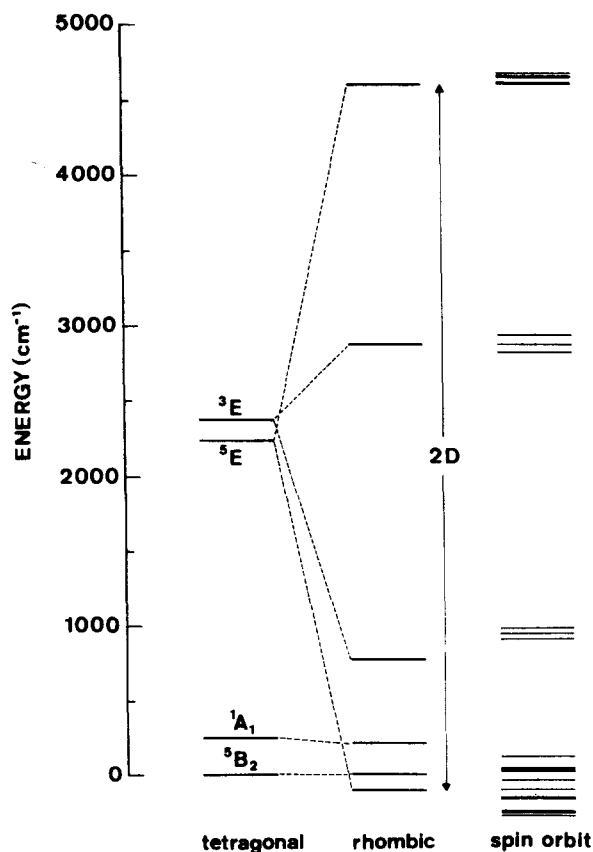


FIG. 6. Relative energies of the low-lying electronic levels of the Fe(II) ion in the $[\text{Fe}(5'\text{-GMP})(\text{H}_2\text{O})_5] \cdot 2\text{H}_2\text{O}$ complex, as obtained from the fitting procedure.

logical systems such as deoxygenated human hemoglobin^{11,12} and sperm whale myoglobin.¹² Likewise in these latter systems, the rhombic distortion makes the 5E level be the ground state after applying the rhombic Hamiltonian. However, the 5E level in the tetragonal symmetry for the Fe(II)-5'-GMP complex lies more than 2000 cm^{-1} above the 5B_2 ground state, while in the other biological systems, this energy is not greater than 300 cm^{-1} . The large rhombic distortion of -2236 cm^{-1} in the Fe(II)-5'-GMP derivative allows the ferrous ions to have the so-called "biological iron" electronic structure.¹²

It was this similarity in the electronic structure which prompted us to study the dynamical properties of the Fe(II)-5'-GMP complex in order to continue the comparison with these biological systems.

V. DYNAMICAL PROPERTIES

Information about some dynamical aspects of the Fe(II)-5'-GMP molecule can be extracted from the variation with temperature of some Mössbauer parameters such as the second-order Doppler shift¹⁹ and the Lamb-Mössbauer factor.²⁰

TABLE IV. Summary of structural and crystal-field data for different systems.

System	$d(\text{Fe-N}_7)$ (Å)	$\epsilon_2(\text{cm}^{-1})$	$\epsilon_3(\text{cm}^{-1})$	$D(\text{cm}^{-1})$	References
Fe(II)-5'-GMP	2.191	11 377	17 747	− 2236	This work
Fe(II)-5'-IMP A ^a	2.243, 2.256	7 303	19 469	− 1098	6,9
B	2.308	4 950	19 562	− 1722	
Deoxy Hb-A ^b	...	8 130	17 180	346	11
	...	9 442	15 881	− 336	12
Deoxy Mb ^b	...	7 907	17 269	− 310	12

^a A and B correspond to the two different Fe(II) sites in the $[\text{Fe}(5'\text{-GMP})(\text{H}_2\text{O})_5] \cdot 2\text{H}_2\text{O}$ complex.

^b Deoxy Hb-A: deoxygenated human hemoglobin; deoxy Mb: deoxygenated sperm whale myoglobin.

A. The Lamb-Mössbauer factor

The Lamb-Mössbauer factor is given by

$$f = \exp(-\langle x^2 \rangle k^2) \quad (13)$$

and it represents the probability for recoil-free absorption. In this equation, k is the wave vector of the gamma radiation and $\langle x^2 \rangle$ is the mean-square amplitude of vibration of the absorbing atom in the γ -ray direction. It is the temperature dependence of $\langle x^2 \rangle$ which allows us to get information about nuclear motion studying $f(T)$ experimental data.

Considering the Debye model of solids, the following form for the f factor is deduced:

$$\ln f = \left\{ \frac{3}{4} \frac{E_\gamma^2}{Mc^2 k_B \theta_D} \left[1 + 4(T/\theta_D)^2 \int_0^{\theta_D/T} \frac{x dx}{e^x - 1} \right] \right\}, \quad (14)$$

where θ_D is the Debye temperature of the solid, M is the effective mass of the iron nucleus, and E_γ is the energy of the γ rays. In the high-temperature limit, Eq. (14) can be written as

$$\ln f = - \frac{3E_\gamma^2}{Mc^2 k_B \theta_D^2} T, \quad (15)$$

where all but the linear term in T have been ignored. The product between the linewidth at half height Γ and the relative line intensity I is proportional to the area under the resonance curve, and consequently to the recoil-free fraction f . Thus, the temperature dependence of the logarithm of the product of Γ and I is the same as that of the logarithm of f . Figure 7 shows the linear dependence of $-\ln(\Gamma \cdot I)$ with temperature for the Fe(II)-5'-GMP complex in the 300–70 K range, indicating that we are situated in the high-temperature limit and therefore Eq. (15) can be applied.

If we assume a value of $0.057 \text{ kg mol}^{-1}$ for the effective mass of the iron nucleus, a Debye temperature of $\theta_D = 185 \text{ K}$ is obtained from the slope of the straight line. This Debye temperature is slightly lower than that calculated from the temperature dependence of the second-order Doppler shift in deoxygenated sperm whale myoglobin $\theta_D = 220 \text{ K}$.¹⁹ This result suggests that the Fe(II) ions are not as rigidly bonded in the Fe(II)-5'-GMP complex as in deoxygenated sperm whale myoglobin.

B. Second-order Doppler shift (SODS)

In order to confirm the Debye temperature θ_D obtained from the temperature dependence of the Lamb-Mössbauer

factor and the effective iron mass value ($M_{\text{Fe}} = 0.057 \text{ kg mol}^{-1}$) assumed in the previous section, we have studied the thermal variation of the isomer shift.

The observed total shift δE_T in the position of a Mössbauer line for the case of source at constant temperature ($T_0 = 298 \text{ K}$) can be written as

$$\delta E_T(T) = \delta E_{\text{iso}}^{\text{Rh}}(T_0) + \delta E_{\text{SODS}}^{\text{Rh}}(T_0) + \delta E_{\text{iso}}^{\text{complex}}(T) + \delta E_{\text{SODS}}^{\text{complex}}(T). \quad (16)$$

Here, $\delta E_{\text{iso}}^{\text{Rh}}(T_0) + \delta E_{\text{iso}}^{\text{complex}}(T)$ gives the isomer shift between the $^{57}\text{CoRh}$ source and the Fe(II)-5'-GMP complex absorber. This mismatch in energy is due to the different chemical environments around the iron nucleus in the source and in the absorber, which cause different electron densities near the nucleus. If the electronic level scheme presents low-lying levels which can be thermally populated in the temperature range of investigation, such as in our case, the isomer shift becomes temperature dependent. The $\delta E_{\text{SODS}}(T)$ terms account for the second-order Doppler shift with respect to a hypothetical environment of rigidly fixed iron atoms. This last contribution to the total isomer shift arises from the thermal vibration of the iron atoms. Assuming that at a given temperature the displacements occur periodically with a mean-squared velocity $\langle u^2 \rangle$, the second-order Doppler shift is given by

$$\delta E_{\text{SODS}} = -E_\gamma \frac{\langle u^2 \rangle}{2c^2}. \quad (17)$$

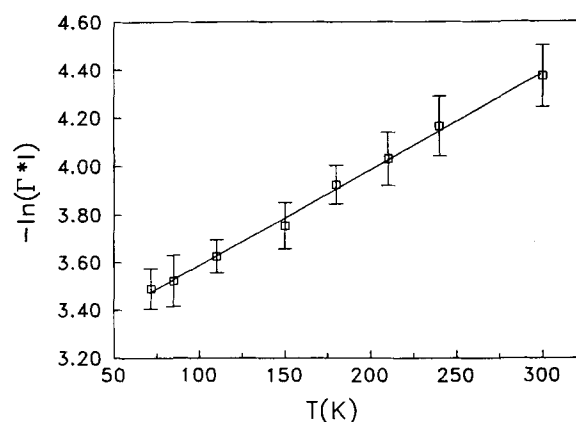


FIG. 7. Temperature dependence of the negative logarithm of the product between the linewidth at half-height and the relative line intensity for the $[\text{Fe}(5'\text{-GMP})(\text{H}_2\text{O})_5] \cdot 2\text{H}_2\text{O}$ complex. The solid line represents the best fit to a straight one.

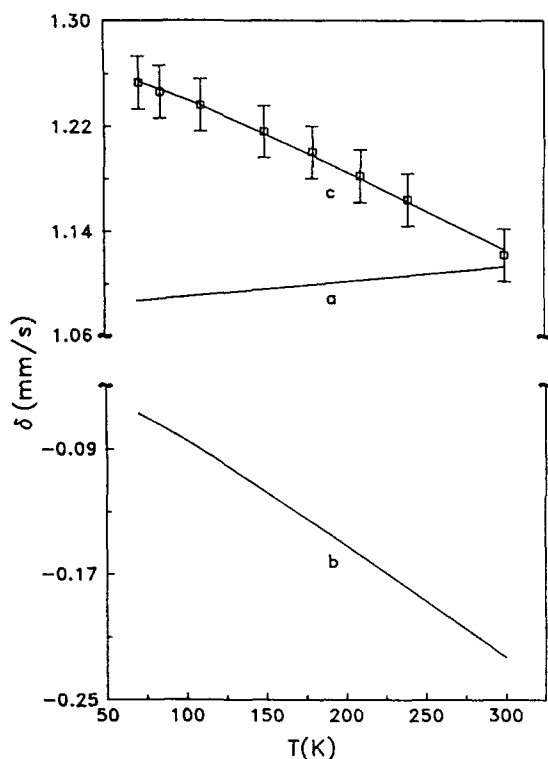


FIG. 8. Interpretation of the temperature dependence of the total Mössbauer isomer shift for the $[\text{Fe}(\text{5'-GMP})(\text{H}_2\text{O})_5] \cdot 2\text{H}_2\text{O}$ complex with the source at room temperature. According to Parak *et al.* (Ref. 19), a linear temperature dependence for the isomer shift of the $\text{Fe}(\text{II})$ -5'-GMP derivative has been assumed (curve a). Curve b gives the second-order Doppler shift of the complex as a function of temperature with $\theta_D = 185$ K and $M_{\text{Fe}} = 0.057$ kg mol $^{-1}$. These two curves along with a constant second-order Doppler shift of the source $\delta_{\text{SODS}}^{\text{Rh}} = +0.236$ mm s $^{-1}$ (Ref. 19) yield the solid line c, which represents a least-squares fit to the experimental data.

The second-order Doppler shift is temperature dependent since $\langle u^2 \rangle$ is proportional to the mean kinetic energy which increases with temperature.

In a Debye model, the mean-square velocity $\langle u^2 \rangle$ is obtained from

$$\langle u^2 \rangle = \left\{ \frac{9R}{8M_{\text{Fe}}c^2} \left[\theta_D + 8T(T/\theta_D)^3 \int_0^{\theta_D/T} \frac{x^3 dx}{e^x - 1} \right] \right\}. \quad (18)$$

As a result, the second-order Doppler shift for the $\text{Fe}(\text{II})$ -5'-GMP complex in the range of temperatures under investigation can be calculated from Eqs. (17) and (18) using the value of the Debye temperature ($\theta_D = 185$ K) obtained from the Lamb-Mössbauer factor and the same effective mass for the iron (curve b of Fig. 8). The corresponding second-order Doppler shift for the source $\delta E_{\text{SODS}}^{\text{Rh}}(T_0)$ has been evaluated by Parak *et al.*¹⁹ and it results to be $+0.236$ mm s $^{-1}$ in units of Doppler velocity. The $\delta E_{\text{iso}}^{\text{complex}}(T)$ may be determined from the energy-level scheme of the iron nucleus (Fig. 6), but in the case of ^{57}Fe , no sufficiently accurate theory exists to enable calculation of absolute values of

the isomer shift from the electronic level scheme. Like Parak *et al.*¹⁹, we have assumed a linear temperature dependence for the isomer shift of the $\text{Fe}(\text{II})$ -5'-GMP complex in the range of temperatures studied. Finally, as $\delta E_{\text{iso}}^{\text{Rh}}(T_0)$ is constant, it can be included in the constant term of the linear variation of $\delta E_{\text{iso}}^{\text{complex}}(T)$.

Figure 8 shows a least-squares fit of the experimental data (line c) using Eq. (16). Only the slope and the constant term of the straight line (a) accounting for $\delta E_{\text{iso}}^{\text{Rh}}(T_0) + \delta E_{\text{iso}}^{\text{complex}}(T)$ were varied. The parameters obtained from the least-squares fitting are in good agreement with those found in the deoxygenated sperm whale myoglobin system,¹⁹ as could be expected due to the similarity between the electronic structures. Moreover, at room temperature, the second-order Doppler shift of the source and that of the sample cancel each other, being the unique contribution to the total isomer shift $\delta E_{\text{iso}}^{\text{Rh}}(T_0) + \delta E_{\text{iso}}^{\text{complex}}(T)$. This fact reduces enormously the set of linear parameters which fit the experimental data.

VI. CONCLUSIONS

The crystal-field parameters obtained from the temperature dependence of both magnetic susceptibility and quadrupolar splitting are in good agreement with the main structural features of the $\text{Fe}(\text{II})$ -5'-GMP molecule. Furthermore, the electronic structure of the $\text{Fe}(\text{II})$ ions is quite similar to those found in some $\text{Fe}(\text{II})$ -containing biological systems such as deoxygenated human hemoglobin^{11,12} and deoxygenated sperm whale myoglobin,¹² which may be indicative of the existence of the so-called "biological" state of the $\text{Fe}(\text{II})$ ion. It may be argued that this electronic structure might be common to the biological systems in which the $\text{Fe}(\text{II})$ ion plays an important role, or even in some of those model systems which try to reproduce more complex real biological situations, as is the case of the $\text{Fe}(\text{II})$ -5'-GMP complex.

The Debye temperature deduced from the Lamb-Mössbauer factor is used to calculate the thermal variation of the second-order Doppler shift which together with a linear temperature dependence for the intrinsic isomer shift, reproduces correctly the experimental data. The Debye temperature is slightly smaller than that found in the deoxygenated myoglobin, but in any case, quite similar. This fact may suggest that in spite of the different size of the two molecules, the iron motion, which is responsible for the effective Debye temperature obtained by Mössbauer spectroscopy, is comparable in the two systems.

ACKNOWLEDGMENTS

This work has received financial support from DGICYT, project number PB86-0074-01, and in part from CIRIT.

¹G. L. Eichhorn, in *Inorganic Biochemistry*, edited by G. L. Eichhorn (Elsevier, Amsterdam, 1973), Vol. 2, pp. 1191-1243; R. B. Martin and H. M. Yitbarek, in *Metal Ions in Biological Systems*, edited by H. Sigel (Marcel Dekker, New York, 1979), Vol. 8, pp. 57-124, *Nucleic Acid-Metal Ion Interactions*, edited by T. G. Spiro (Wiley, New York, 1980), Vol. 1; *Metal-DNA Chemistry*, edited by T. D. Tullius (ACS Symposium Series,

- Washington, 1989), No. 402.
- ²B. Singer, *Biochem. Biophys. Acta* **80**, 137 (1964).
- ³M. J. Cleare and P. C. Hydes, in *Metal Ions in Biological Systems*, edited by H. Sigel (Dekker, New York, 1980), pp. 1–62; E. A. Sausville, J. Peisach, and S. B. Horwitz, *Biochemistry* **17**, 2740 (1978); P. Umapathy, *Coord. Chem. Rev.* **95**, 129 (1989).
- ⁴J. K. Barton, *Comments Inorg. Chem.* **3**, 321 (1985).
- ⁵D. J. Hodgson, *Prog. Inorg. Chem.* **23**, 211 (1977); R. W. Gellert and R. Bau, in *Metal Ions in Biological Systems*, edited by H. Sigel (Marcel Dekker, New York, 1979), Vol. 8, pp. 1–55; V. Swaminathan and M. Sundaralingam, *CRC Crit. Rev. Biochem.* **6**, 245 (1979).
- ⁶M. V. Capparelli, D. M. L. Goodgame, P. B. Hayman, A. C. Skapski, and D. E. Hathway, *FEBS Lett.* **163**, 241 (1983).
- ⁷M. V. Capparelli, D. M. L. Goodgame, P. B. Hayman, and A. C. Skapski, *Inorg. Chem. Acta* **125**, L47 (1986).
- ⁸D. M. L. Goodgame, P. B. Hayman, and I. Sayer, *Inorg. Chem. Acta* **92**, L13 (1984).
- ⁹E. Molins, A. Labarta, J. Tejada, and V. Moreno, *Z. Phys. B* **59**, 419 (1985).
- ¹⁰H. Eicher and A. Trautwein, *J. Chem. Phys.* **50**, 2540 (1969).
- ¹¹B. H. Huynh, G. C. Papaefthymiou, C. S. Yen, J. L. Groves, and C. S. Wu, *J. Chem. Phys.* **61**, 3750 (1974).
- ¹²H. Eicher, D. Bade, and F. Parak, *J. Chem. Phys.* **64**, 1446 (1976).
- ¹³H. A. Tajmir-Riahi and T. Theophanides, *Can. J. Chem.* **61**, 1813 (1983); T. Theophanides and H. A. Tajmir-Riahi, in *Spectroscopy of Biological Molecules*, edited by C. Sandorfy and T. Theophanides (Reidel, Dordrecht, 1984), pp. 137–152.
- ¹⁴F. E. Mabbs and D. J. Machin, *Magnetism and Transition Metal Complexes* (Chapman and Hall, London, 1973), p. 5.
- ¹⁵A. T. Casey and S. Mitra, in *Theory and Applications of Molecular Paramagnetism*, edited by E. A. Boudreaux and L. N. Mulay (Wiley, New York, 1976), pp. 198–203.
- ¹⁶A. Labarta, E. Molins, X. Viñas, J. Tejada, A. Caubet, and S. Alvarez, *J. Chem. Phys.* **80**, 444 (1984).
- ¹⁷T. C. Gibb, *Principles of Mössbauer Spectroscopy* (Wiley, New York, 1976).
- ¹⁸R. M. Sternheimer, *Phys. Rev.* **84**, 244 (1951).
- ¹⁹L. Reinisch, J. Heidemeier, and F. Parak, *Eur. Biophys. J.* **12**, 167 (1985).
- ²⁰R. H. Nussbaum, in *Mössbauer Effect Methodology*, edited by I. J. Gruverman (Plenum, New York, 1966), Vol. 2, pp. 3–21. P. Gülich, R. Link, and A. Trautwein, *Mössbauer Spectroscopy and Transition Metal Chemistry* (Springer, Berlin, 1978).